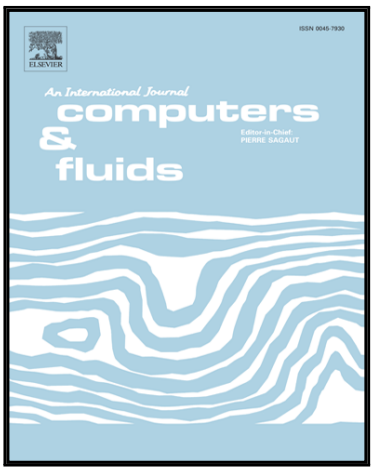

The effect of surface tension on free surface flow induced by a point sink in a fluid of finite depth.

G.C. Hocking, H.H.N. Nguyen, T.E. Stokes, L.K. Forbes

PII: S0045-7930(17)30280-3
DOI: 10.1016/j.compfluid.2017.08.015
Reference: CAF 3570

To appear in: *Computers and Fluids*

Received date: 29 March 2016
Revised date: 14 June 2017
Accepted date: 4 August 2017

Please cite this article as: G.C. Hocking, H.H.N. Nguyen, T.E. Stokes, L.K. Forbes, The effect of surface tension on free surface flow induced by a point sink in a fluid of finite depth., *Computers and Fluids* (2017), doi: 10.1016/j.compfluid.2017.08.015

Highlights

- Maximum flow rate steady solutions for withdrawal through a point sink in water of finite depth computed.
- Different fluid depths, sink depths and flow rates, and the effects of surface tension included.
- Two completely different numerical methods (integral equation and spectral) used and compared.
- Limit as surface tension approaches zero consistent with previous research.

The effect of surface tension on free surface flow induced by a point sink in a fluid of finite depth.

G.C. Hocking[a,*], H.H.N. Nguyen[a], T.E. Stokes[b], L.K. Forbes[c]

[a] *Mathematics and Statistics, Murdoch University, Perth, Western Australia*
[b] *Department of Mathematics, University of Waikato, Hamilton, New Zealand*
[c] *School of Mathematics and Physics, University of Tasmania, Hobart,Australia*

Abstract

Solutions are presented to the problem of steady, axisymmetric flow of an inviscid fluid into a point sink. The fluid is of finite depth and has a free surface. Two numerical schemes, a spectral method and an integral equation approach, are implemented to confirm results for the maximum-flow-rate steady solution for each configuration. The effects of surface tension and sink depth are included and constitute the new component of the work. Surface tension has the effect of increasing the maximum flow rate at which steady-state solutions can exist.

Keywords: Free surface flow, surface tension, point sink.

1. Introduction

The problem of steady flow due to a single, motionless sink beneath a free surface has proven deceptively difficult. More accurately, while it is relatively easy to obtain numerical solutions to this problem, the limiting parameters for which steady flows exist have proven difficult to find with confidence. While it is generally accepted that as the flow rate increases there comes a point beyond

*Corresponding author
Email addresses: G.Hocking@murdoch.edu.au (G.C. Hocking), Ha.Nguyen@murdoch.edu.au (H.H.N. Nguyen), stokes@waikato.ac.nz (T.E. Stokes), Larry.Forbes@utas.edu.au (L.K. Forbes)

which steady solutions no longer exist, this critical value has had multiple proposed values in the literature using similar numerical methods. The current work uses two completely different numerical approaches to resolve the critical values at which steady solutions cease to exist for the flow into a point sink above a horizontal base. The agreement of these two different approaches is central to the conclusions drawn about the solutions. Surface tension is included in the work, both to gauge its influence on the flows and for its stabilizing effect on both the flow and the numerical schemes.

While the results are of mathematical interest as a fundamental study of free surface hydrodynamics, the problem is also relevant to the withdrawal of fluid from water storage reservoirs and other confined water bodies (Imberger & Hamblin (1982); Imberger & Patterson (1990)). Fluid withdrawn from reservoirs tends to flow in layers due to the density stratification inherent in all reservoirs in temperate climatic zones. This vertical stratification often consists of constant density regions and regions with approximately linear density variation due to either temperature or salinity. An understanding of the process of selective withdrawal is important in delivering suitable water quality for urban and agricultural supply.

Peregrine (1972) proposed the analogous problem in two dimensions (with a line sink) as a study that might assist in understanding wave-breaking, and while this has proven not to be the case for steady flow, some wave breaking behaviour has been observed in the unsteady version in which the sink is turned on in a fluid at rest (Stokes et al. (2003)). Regardless, the steady problem with a line sink has provided some very interesting behaviour and due to the (relative) ease of computation and the availability of complex variable methods (Sautreaux (1901); Craya (1940); Peregrine (1972); Tuck & Vanden Broeck (1984); Vanden-Broeck & Keller (1987); Hocking & Forbes (1991); Forbes & Hocking (1993)) there has been much work on this case. Surface

tension was considered in Forbes & Hocking (1993), and withdrawal in the presence of a background flow by Holmes & Hocking (2015). In both cases non-uniqueness was found in the solution space. Two kinds of steady solution were obtained for flow from a single layer fluid with a free surface, one involving a stagnation point on the surface and another involving a cusp above the sink (Sautreaux (1901); Tuck & Vanden Broeck (1984); Vanden-Broeck & Keller (1987)). Hocking (1995) and Hocking & Forbes (2001) showed that the cusp solutions correspond to the situation in which the free surface is pulled down directly into the sink if the withdrawal rate is increased beyond this value. Thus, if there is another fluid above this layer, this flow corresponds to the transition to a two-layer flow in which fluid from both layers flow out through the sink. This was found to be true in both an unconfined fluid and a fluid of finite depth. Numerical calculations of the unsteady flow indicate that this critical drawdown flow is related to the maximum steady flow, but the actual drawdown of the interface between two layers occurs at a flow rate that depends on the flow history (Stokes et al. (2003, 2008)).

This considerable progress in the two dimensional case has not really been matched in the problem of flow due to a point sink. Such flows were considered experimentally by Harleman et al. (1959); Jirka & Katavola (1979); Lubin & Springer (1967) and others, and later in a full simulation by Zhou & Graebel (1990) and Xue & Yue (1998). Miloh & Tyvand (1993) considered a small time expansion to look for critical drawdown values. No solutions with the equivalent of a cusp shape have been found, except over a small range of parameters (Forbes & Hocking (2003)).

The first computations of steady solutions for a point sink with a stagnation point were performed by Forbes & Hocking (1990) and Vanden-Broeck & Keller (1997) on the case of a semi-infinite fluid. These authors solved the same equations but using different numerical approaches. The problem can

be defined in terms of a Froude number $F_S = \sqrt{m^2/(gH_S^5)}$, where m is the sink strength, g is gravitational acceleration and H_S is the depth of the sink. While the former found a limiting value of $F_S \approx 6.4$, the latter obtained values close to $F_S = 5.4$ (with a train of decaying upstream waves) using essentially the same integral equation approach. The limiting solutions in both cases appeared to have the same physical characteristic of a stagnation ring on the free surface some small distance from the central surface stagnation point. Solutions were computed using integral equation techniques pushing the limits of computer power of the time. Similar discrepancies in the critical values appeared when a flow with the sink on a horizontal, impermeable base were computed by Hocking et al. (2002) (using the numerical approach of Vanden-Broeck & Keller (1997)) who found $F_S \approx 3.24$, while Forbes et al. (1996) obtained a much lower value of $F_S \approx 1.5$ using a fundamental singularity, Galerkin technique. The former contained the familiar stagnation ring limiting solution, but the latter did not. Experiments and full numerical simulations in various geometries produced values for limiting single layer flows ranging from $F_S \approx 1.6$ (Harleman et al. (1959)) to $F_S \approx 3$ (Zhou & Graebel (1990)) although these may not be directly related to limiting steady-state solutions with a central stagnation point.

A recent, more thorough analysis of the integral equation method was given in Hocking et al. (2014), and it was shown that the limiting steady solutions occur at much lower values of flow rate than initial calculations suggest. Surface tension was included in Hocking et al. (2015) and was found to have a regularizing effect on both the solutions and the existence space, so that much higher flow rates could be obtained with significant surface tension included. The "errors" appear to be due to inappropriate truncation Forbes & Hocking (1990) and lack of convergence of the numerical scheme as grid spacing was decreased Vanden-Broeck & Keller (1997), but in both cases this was not

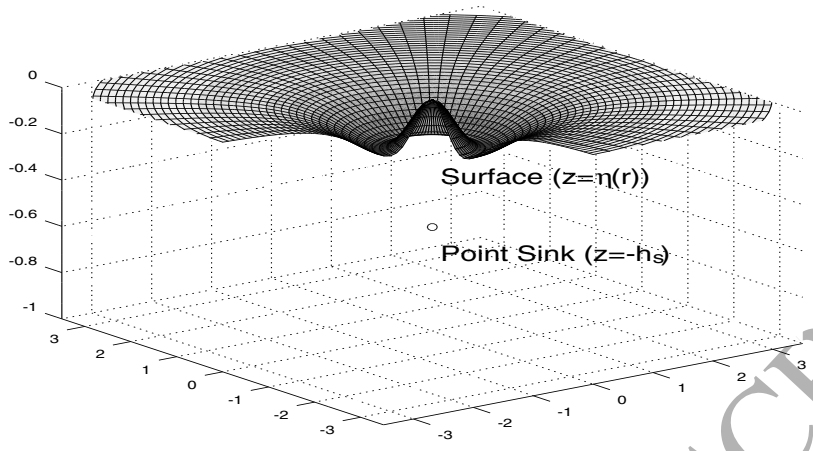

Figure 1: Cut-out sketch of a typical axi-symmetric surface shape, $z = \eta(r)$. The fluid is of finite depth and withdrawal is through a point sink situated at depth $z = -h_S$.

obvious with the computational capacity available at the time.

Here we consider the problem with a point sink situated at an arbitrary depth in a fluid of finite depth and include the effects of surface tension, see Figure 1. Two different numerical schemes are used and found to give matching solutions for all parameter values. Again, the effect of surface tension is to regularize the flow. By taking the limit as the surface tension approaches zero we are able to confirm the limiting values for zero surface tension.

2. Problem Formulation

Consider the steady, irrotational, axisymmetric flow of an inviscid, incompressible fluid beneath a free surface. The flow is driven by a point sink of strength m situated at a depth H_S beneath the undisturbed level of the free surface and above a flat impermeable boundary at depth D. Under these assumptions the problem can be formulated in terms of a velocity potential $\phi(r, z)$, where r is a radial coordinate centred on the location of the point sink and z is the vertical coordinate with $z = 0$ corresponding to the level of the free

surface if there is no flow. Thus the velocity can be obtained as $\nabla\phi = (u, w)$, where u is the radial component and w is the vertical component. The free surface is subject to surface tension, T.

Nondimensionalising the potential and length with respect to (m/D) and D respectively, where the quantity m is the strength of the point sink, the problem is to solve

$$\nabla^2\phi = 0, \quad -1 < z < \eta(r), \quad (r, z) \neq (0, -h_S), \tag{1}$$

subject to the dynamic condition obtained from setting pressure to the atmospheric value on the free surface in the Bernoulli equation, i.e.

$$\eta + \frac{F_D^2}{2}(u^2 + w^2) - \frac{\beta\left(r\eta_{rr} + \eta_r(1 + \eta_r^2)\right)}{r[1 + \eta_r^2]^{3/2}} = 0 \quad \text{on} \quad z = \eta(r) \tag{2}$$

with a kinematic condition that no flow can occur through the surface in steady flow given by

$$\nabla\phi \cdot \mathbf{n} = \phi_r\eta_r - \phi_z = 0 \quad \text{on} \quad z = \eta(r), \tag{3}$$

where $\mathbf{n}$ is the normal to the free surface, and a condition that there can be no flow through the impermeable base beneath the layer of fluid,

$$\phi_z = 0 \quad \text{on} \quad z = -1. \tag{4}$$

These equations include the main parameters that control this flow; the Froude number, the sink depth and the surface tension

$$F_D = \left(\frac{m^2}{gD^5}\right)^{1/2}, \quad h_S = H_S/D, \quad \beta = \frac{T}{gD^2} \tag{5}$$

in which g is gravitational acceleration. In most cases the Froude number can be thought of as an effective flow rate. We can define a second Froude number that is based on the depth of the sink rather than the depth of the fluid as

$$F_S = \left(\frac{m^2}{gH_S^5}\right)^{1/2}. \tag{6}$$

The value of F_S is related to F_D via the relation $F_D = h_S^{5/2} F_S$, where h_S is the nondimensional sink depth, and is useful for comparison with values computed in an unbounded fluid, for which $F_D \to 0$ as $D \to \infty$.

In the limit as we approach the point sink at $(r, z) = (0, -h_S)$ the velocity potential should take the form

$$\Phi_S \to \frac{1}{4\pi\sqrt{r^2 + (z + h_S)^2}} \tag{7}$$

which corresponds to a total flux into the sink of $Q = 4\pi$. A change of sign reverses the flow direction from a sink flow to a source flow. However, in the case of steady flow, the quadratic nature of the velocity term in the dynamic condition (2) means that steady solutions are valid for both a source and a sink.

3. Rigid-lid solution

It is of interest to compute a solution that is valid for small flow rates that result in a small disturbance to the free surface. In essence we can compute the flow due to a point sink confined in a horizontal duct. An expansion about the flow along the top of the duct is used to approximate the shape of the free surface. The linearized problem is thus to solve Laplace's equation in the region $-1 < z < 0$ subject to the linearized kinematic conditions of $\phi_z = 0$ on $z = 0, -1$. The dynamic condition (2) can then be used to estimate the shape of the free surface by expanding about $z = 0$. Following the usual procedure of allowing $\phi = \phi_0 + \phi_1 + \ldots$ and $\eta = 0 + Z_1(r) + \ldots$ we can choose,

$$\phi_0(r, z) = \frac{1}{4\pi R_1} + \frac{1}{4\pi R_2} + \int_0^\infty a(k) \cosh k(z + 1) J_0(kr) dk, \quad z \le \eta(r) \tag{8}$$

where $a(k)$ is a real function to be determined. The terms involving $R_1 = [r^2 + (z + h_S)^2]^{1/2}$ and $R_2 = [r^2 + (z + 2 - h_S)^2]^{1/2}$ represent a point sink at $z = -h_S$ and an image (about the base) at $z = -2 + h_S$. This choice

satisfies the sink behaviour (7), the condition of an impermeable boundary on the bottom (4) and also satisfies Laplace's equation (1), and so it remains to satisfy the free surface conditions (2),(3).

At leading order the kinematic condition on $z = 0$, gives

$$\begin{aligned}\phi_{0z}(r,0) &= -\left[\frac{z+h_S}{4\pi R_1^3} + \frac{z+2-h_S}{4\pi R_2^3} + \int_0^\infty a(k)k\sinh k(z+1)J_0(kr)dk\right]_{z=0} = 0,\\ &= -\frac{h_S}{4\pi(r^2+h_S^2)^{3/2}} - \frac{2-h_S}{4\pi(r^2+(2-h_S)^2)^{3/2}} + \int_0^\infty a(k)k\sinh kJ_0(kr)dk = 0\end{aligned} \tag{9}$$

This equation can be solved using Hankel transforms; noting that

$$\int_0^\infty e^{-ck}J_0(kr)kdk = \frac{c}{(c^2+r^2)^{3/2}} \tag{10}$$

we find that

$$a(k) = \frac{e^{-h_S k} + e^{-(2-h_S)k}}{4\pi\sinh k} \tag{11}$$

and so the full form of the linear solution for ϕ_0 in a duct is (8) with this form (11) for $a(k)$.

The remaining condition is the dynamic condition, (2), which linearizes to

$$\beta Z_1''(r) + \frac{\beta}{r}Z_1'(r) - Z_1(r) = G(r) \tag{12}$$

where $Z_1(r)$ is the first-order perturbation to $z = \eta(r)$ and $G(r) = \frac{F_D^2}{2}\phi_{0r}^2(r,0)$ is the velocity along the top surface computed from (8). The solution of this differential equation provides the "rigid-lid" solution for flow due to a point sink in water of finite depth. If there is no surface tension, then the solution becomes simply

$$Z_1(r) = -\frac{F_D^2}{2}\phi_{0r}^2(r,0). \tag{13}$$

In the case of non-zero surface tension, the equation can be solved using Hankel transforms, or by noting that from Bessel's differential equation,

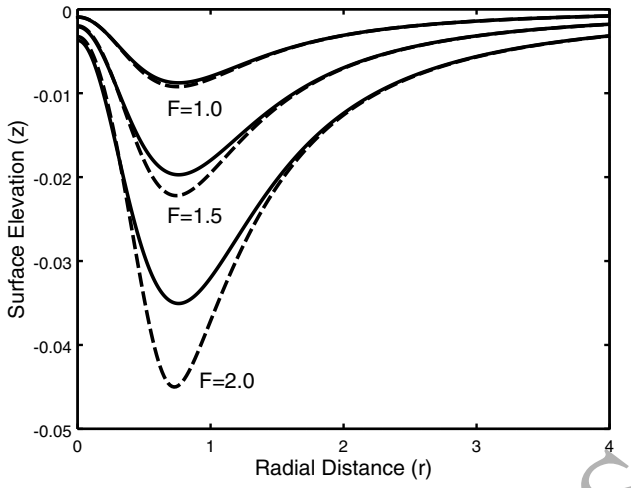

Figure 2: Rigid lid solution compared with full nonlinear solution for $\beta = 0.005$ with $F = 1, 1.5$ and 2.0. The solid line is the approximate solution in each case. The effect of nonlinearity is clear in each, pulling the surface down more sharply. The sink is located on the base at $z = -1$.

$J_0''(y) + \frac{1}{y}J_0'(y) = -J_0(y)$, so that if

$$Z_1(r) = \int_0^\infty A(k)J_0(kr)kdk \tag{14}$$

then

$$\int_0^\infty (-1 - \beta k^2)A(k)kJ_0(kr)dk = G(r) \tag{15}$$

and inverting the Hankel Transform

$$A(k) = \frac{-1}{1+\beta k^2}\int_0^\infty G(r)J_0(kr)rdr. \tag{16}$$

The solution for $Z_1(r)$ is therefore given by (14) with $A(k)$ given by (16). Unfortunately, these integrals cannot be completely evaluated in closed form, but it is a straightforward matter to compute them using quadrature. An example is given in Figure 2 which shows several comparisons of the rigid-lid solution with the full nonlinear solution for the case of a sink on the bottom at $z = -1$ and a surface tension value of $\beta = 0.005$ for $F_S = 1.0, 1.5$ and 2.0.

Solutions with smaller values of F_S are graphically identical to the nonlinear solutions. The limiting (nonlinear solution) value is $F_S = 2.33$ for this case. Higher flow rates (F_S) result in a deeper dip and it is clear that the effect of nonlinearity is to pull the surface even deeper. However, for reasonable values of F_S and β the comparison is good, giving us the confidence to proceed with the full nonlinear solutions.

4. The numerical methods

To consider the full nonlinear steady flow problem we need to implement a numerical scheme. Given the range of different critical values of Froude number obtained using different methods (Forbes & Hocking (1990); Forbes et al. (1996); Vanden-Broeck & Keller (1997); Hocking et al. (2002)), we consider two completely different approaches. First, we implement a spectral representation of the flow based on an extension of the rigid-lid solution, using an iterative scheme to compute the series coefficients. In addition, we use an approach similar to that of Forbes & Hocking (1990); Vanden-Broeck & Keller (1997) and Hocking et al. (2002). The flow is assumed to be axisymmetric and an integral equation is derived for the elevation and velocity potential on the free surface.

4.1. Spectral Method

We extend the rigid-lid approach above by allowing the free surface to "move". To do this we define the same potential function that satisfies all but the free surface conditions given in (8). The difference in this section is that $\phi(r, z)$ will now be evaluated at points directly on the free surface.

As above, this choice satisfies the sink behaviour (7), the condition of an impermeable boundary on the bottom (4) and Laplace's equation (1) everywhere except at the sink, and so it remains to satisfy the free surface conditions (2),(3).

It is possible to continue the derivation using the continuous form of ϕ, but ultimately it will be necessary to truncate the integral in order to complete the numerical solution, and so we continue from here using the discrete form of the truncated integral,

$$\phi(r,z) = \frac{1}{4\pi R_1} + \frac{1}{4\pi R_2} + \sum_{j=0}^{\infty} a_j \cosh \lambda_j (z+1) J_0(\lambda_j r), \quad z \le \eta(r), 0 < r < L \tag{17}$$

where a_j are real coefficients to be computed, $\lambda_j, j = 1, 2, \ldots$ are appropriate eigenvalues, and $J_0(\lambda_j r)$ is the first-kind Bessel function. This also satisfies all of the conditions except those on the free surface (2),(3). The truncation point, L, is chosen to be large enough to provide converged solutions. The eigenvalues are chosen so that $J_0(\lambda_k L) = 0$. This choice makes no difference to the computed solutions (see below) because $\phi \to 0$ as $r \to \infty$.

Using this ϕ we can now compute the velocity components at any point on the free surface $z = \eta(r)$ as

$$\begin{aligned} u = \phi_r(r,\eta) = & - \frac{r}{4\pi[r^2 + (\eta(r) + h_S)^2]^{3/2}} - \frac{r}{4\pi[r^2 + (\eta(r) + 2 - h_S)^2]^{3/2}} \\ & - \sum_{j=1}^{\infty} a_j \lambda_j \cosh \lambda_j (\eta(r) + 1) J_1(\lambda_j r) \end{aligned} \tag{18}$$

$$\begin{aligned} w = \phi_z(r,\eta) = & - \frac{\eta(r) + h_S}{4\pi[r^2 + (\eta(r) + h_S)^2]^{3/2}} - \frac{\eta(r) + 2 - h_S}{4\pi[r^2 + (\eta(r) + 2 - h_S)^2]^{3/2}} \\ & + \sum_{j=1}^{\infty} a_j \lambda_j \sinh \lambda_j (\eta(r) + 1) J_0(\lambda_j r) \end{aligned} \tag{19}$$

where $J_1(\lambda_j r)$ is the first-kind Bessel function, noting that $J_0'(x) = -J_1(x)$ (Abramowitz & Stegun (1970)).

We also define

$$\eta(r) = Z_1(r) + \sum_{j=1}^{\infty} c_j J_0(\lambda_j r) \tag{20}$$

where the $c_j, j = 1, 2, \ldots$ are to be determined and $Z_1(r)$ is the rigid-lid solution computed above. Note that it is necessary that $\eta(r) - 2\beta\eta''(r) \to 0$

as $r \to 0$, to satisfy the condition (2).

At this point we might expect that we could substitute these series into (3) and (2) and solve for the series coefficients using Newton's method with collocation at points on the free surface. However, this procedure proves to be highly ill-conditioned. An approach that works is to exploit the orthogonality of the eigenfunctions involved in each equation, producing an equation for each of the series coefficients. These equations are nonlinear but can still be solved by an iterative method and prove to give a much better conditioned system.

The equation (2) can be modified by invoking the orthogonality of the eigenfunctions to give an equation for the coefficients. Substituting the series form for $\eta(r)$ into (2),

$$\sum_{k=0}^{\infty} c_k J_0(\lambda_k r) = -Z_1(r) - \frac{F_D^2}{2}(\phi_r^2 + \phi_z^2) + \frac{\beta\left(r\eta'' + \eta'(1+\eta'^2)\right)}{r[1+\eta'^2]^{3/2}}, \tag{21}$$

and then using orthogonality of the Bessel functions, we find an expression for the coefficients c_k as

$$c_k = \frac{2}{L^2 J_1^2(\lambda_k)} \int_0^L \left[-Z_1(r) - F_D^2(\phi_r^2 + \phi_z^2) + \frac{\beta\left(r\eta'' + \eta'(1+\eta'^2)\right)}{r[1+\eta'^2]^{3/2}} \right] r J_0(\lambda_k r) dr, \tag{22}$$

$k = 1, 2, 3, \ldots, N$ where L is the truncation point and $\lambda_k, k = 1, 2, \ldots$ are the appropriate eigenvalues of J_0 for this value of L. The other condition (3) can be dealt with similarly, but one must be careful because the hyperbolic sine and cosine terms (which make the orthogonality inviolate) cannot be ignored and consequently we add and subtract terms so that the resulting equations for $a_k, k = 1, 2, \ldots$ are

$$a_k \lambda_k - \frac{2}{L^2 J_1^2(\lambda_k L)} \int_0^L \left[a_k \lambda_k (1 + \sinh \lambda_k (\eta + 1)) + (\phi_z - \eta'(r)\phi_r) \right] J_0(\lambda_k r) r dr = 0, \tag{23}$$

for $k = 1, 2, 3, \ldots$.

The series can be truncated after N terms, giving $2N$ unknowns in $c_k, a_k, k = 1, 2, 3, \ldots, N$. An initial guess for the coefficients was then given and the so-

lution to the set of $2N$ nonlinear equations in $2N$ unknowns was determined via Newtonian iteration using the `fsolve` routine in `Octave` (or `Matlab`). The integrals can be calculated very accurately using Gaussian quadrature, and so it is only choices of L and N that determine the accuracy of the solution. Care must be taken in computing the series terms because for large N the eigenvalues can become very large and finding the hyperbolic sine and cosine terms can cause floating point errors.

Results were found to be converged with $N = 320$, being graphically identical to those with $N = 200$, and the maximum Froude number computed was found to be accurate to two decimal places, except for very small surface tension values. The choice of L was found to give consistent results once $L > 8$ with the sink on the bottom of the channel, but smaller values were found to be sufficient as the sink moved closer to the free surface as the radial disturbance to the free surface was found to be proportional to the depth of the sink, h_S.

4.2. Integral Equation

The formulation of the second numerical scheme follows that given in Forbes & Hocking (1990), Vanden-Broeck & Keller (1997) and Hocking et al. (2002). We use Green's second identity to derive an integral equation for the unknown analytic function $\Phi(r, z)$ and surface elevation, $z = \eta(r)$. Let Q be a fixed point on the free surface with coordinates $(r, \theta, \eta(r))$ and $P(\gamma, \beta, \mu)$ be another point which is free to move over the same surface. An efficient way to satisfy the bottom boundary condition (4) is to place an image free surface at $z \approx -2$ and an image point sink at $z = -(2 - h_S)$. Since Φ is an analytic function over the full region except at the sink itself, we can define another function $\Psi = 1/R_{PQ}$ which is also analytic except when P and Q are the same point, i.e.,

$$\Psi = \frac{1}{R_{PQ}} = \frac{1}{[r^2 + \gamma^2 - 2r\gamma\cos(\beta - \theta) + (z - \mu)^2]^{1/2}} \tag{24}$$

so that we can invoke Green's second identity to obtain

$$\int\int_{\partial V} \left[\Phi \frac{\partial \Psi}{\partial n} - \Psi \frac{\partial \Phi}{\partial n}\right] dS = 0 \tag{25}$$

where n denotes the outward normal direction, and ∂V consists of the free surface S_T and it's image S_B, with the point Q carefully excluded by a small hemispherical surface, S_Q, and small spheres about the sink and its image, S_{ϵ_1}, S_{ϵ_2}.

It is not difficult to show that the contributions from all of these surfaces leads to an integral equation of the form

$$\begin{aligned} 2\pi\Phi(Q) = &\frac{1}{(r^2 + (z + h_S)^2)^{1/2}} + \frac{1}{(r^2 + (z + (2 - h_S))^2)^{1/2}} \\ &- \int\int_{S_T} \Phi(P) \frac{\partial}{\partial n_P}\left(\frac{1}{R_{PQ}}\right) dS_P - \int\int_{S_B} \Phi(P) \frac{\partial}{\partial n_P}\left(\frac{1}{R_{PQ}}\right) dS_P. \end{aligned} \tag{26}$$

Note that (from Hocking et al. (2002))

$$\int\int_{S_T} \frac{\partial}{\partial n_P}\left(\frac{1}{R_{PQ}}\right) dS_P = 0 \tag{27}$$

and therefore we can write equation (26) in the form

$$\begin{aligned} 2\pi\Phi(Q) = &\frac{1}{(r^2 + (z + h_S)^2)^{1/2}} + \frac{1}{(r^2 + (z + 2 - h_S)^2)^{1/2}} \\ &- \int\int_{S_T} [\Phi(P) - \Phi(Q)] \frac{\partial}{\partial n_P}\left(\frac{1}{R_{PQ}}\right) dS_P - \int\int_{S_B} \Phi(P) \frac{\partial}{\partial n_P}\left(\frac{1}{R_{PQ}}\right) dS_P. \end{aligned} \tag{28}$$

This form turns out to be both accurate and stable numerically, enabling us to compute solutions for the full nonlinear flow problem (when such solutions exist).

Following Forbes & Hocking (1990) and Hocking et al. (2002), the surface

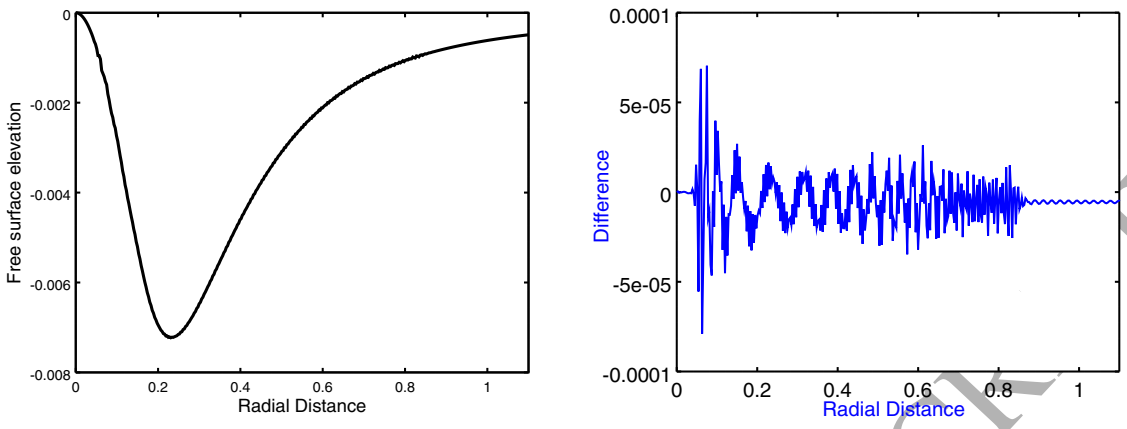

Figure 3: Comparison of "limiting" solutions with zero surface tension. The left panel shows the integral equation solution while the right panel shows the difference between this and the spectral solution. The regular oscillations are from the form of the spectral solution, while numerical instabilities are evident as the more violent oscillations. These instabilities are most evident in the dip region $0.05 < r < 0.8$. Here, $F_D = 0.2, F_S = 3.1$ and $h_S = 1/3$. The figure is scaled so that the sink is located at $z = -1$ and the base is at $z = -3$.

integral can be specified in terms of the variables of the problem as

$$2\pi\Phi(Q) = \frac{1}{(r^2+(z+h_S)^2)^{1/2}} + \frac{1}{(r^2+(z+2-h_S)^2)^{1/2}} - \int_0^\infty (\Phi(P)-\Phi(Q))\mathcal{K}(a,b,c,d)d\rho - \int_0^\infty \phi(P)\mathcal{K}(e,b,f,d)d\rho \tag{29}$$

in which the kernel function is

$$\mathcal{K}(a,b,c,d) = \gamma \int_0^{2\pi} \frac{a - b\cos(\beta-\theta)}{[c - d\cos(\beta-\theta)]^{3/2}} d\beta \tag{30}$$

and the intermediate quantities $a - f$ are defined as

$$a = \gamma\eta_\gamma(P) - (\eta(P)-\eta(Q)), \qquad b = r\eta_\gamma(P) \tag{31}$$

$$c = \gamma^2 + r^2 + (\eta(P)-\eta(Q))^2, \qquad d = 2r\gamma \tag{32}$$

$$e = \gamma\zeta_\gamma(P) - (2+\eta(P)+\eta(Q)), \qquad f = \gamma^2 + r^2 + (2+\eta(P)+\eta(Q))^2 \tag{33}$$

Forbes & Hocking (1990) reduced this to the form

$$\mathcal{K}(a,b,c,d) = \frac{2}{\sqrt{c+d}}\left[\eta_\gamma K\left(\frac{2d}{c+d}\right) + \left(\frac{2ar - \eta_\gamma c}{c-d}\right) E\left(\frac{2d}{c+d}\right)\right] \tag{34}$$

where K and E are the complete elliptic integrals of the first and second kind as defined in Abramowitz & Stegun (1970). At this point we note that E is well-behaved over the interval of interest, but that K has a logarithmic singularity as $P \to Q$, in the integral over the free surface.

This problem was solved using a formulation based on arclength along the surface, so that s is the distance from $\gamma = 0$ to Q, and σ is the distance along the surface to P. The standard formula

$$\left(\frac{dr}{ds}\right)^2 + \left(\frac{d\eta}{ds}\right)^2 = 1 \tag{35}$$

defines the arclength s in terms of r and η. We define a surface potential $\phi(s)$, and applying the chain rule, we find that along the surface,

$$\frac{\partial \phi}{\partial r} = \Phi_r(r,\eta) + \Phi_z(r,\eta)\frac{d\eta}{dr}. \tag{36}$$

Eliminating Φ_z from the Bernoulli equation (2) and the kinematic condition (3) and combining leads to a single relation,

$$\frac{1}{2}F_D^2\left(\frac{d\phi}{ds}\right)^2 + \eta(s) - \beta\left(\frac{\eta''(s)}{r'(s)} + \frac{\eta'(s)}{r(s)}\right) = 0, \tag{37}$$

on the free surface $z = \eta(r)$.

Rewriting the integral equation in terms of arclength, we obtain

$$\begin{aligned} 2\pi\phi(s) = {} & \frac{1}{(r^2(s) + (\eta(s)+1)^2)^{1/2}} + \frac{1}{(r^2(s) + (\eta(s)+2-h_S)^2)^{1/2}} \\ & - \int_0^\infty (\phi(\sigma) - \phi(s))\,\mathcal{K}(A,B,C,D)d\sigma \\ & - \int_0^\infty \phi(\sigma)\mathcal{K}(E,B,F,D)d\sigma, \end{aligned} \tag{38}$$

where

$$\begin{aligned} A &= r(\sigma)\eta'(\sigma) - r'(\sigma)(\eta(\sigma) - \eta(s)), & B &= r(s)\eta'(\sigma) \\ C &= r^2(\sigma) + r^2(s) + (\eta(\sigma) - \eta(s))^2, & D &= 2r(s)r(\sigma) \\ E &= r(\sigma)\eta'(\sigma) - r'(\sigma)(2 + \eta(\sigma) + \eta(s)), \\ F &= r^2(\sigma) + r^2(s) + (2 + \eta(\sigma) + \eta(s))^2. \end{aligned} \tag{39}$$

This integral equation is coupled with the condition (35), subject to (37) to give the complete formulation of the problem.

These equations were solved numerically using collocation. A grid of points was chosen at arclength values $s = s_0, s_1, s_2, s_3, \ldots, s_N$. An initial guess for the surface shape $\eta = \eta_0, \eta_1, \eta_2, \ldots, \eta_N$ and potential function $\phi = \phi_0, \phi_1, ..., \phi_N$ was made and used to compute the error in the integral equation (38) and the condition on the surface (37). All integration was conducted using cubic splines, but the results were identical if a much simpler trapezoidal rule was used. The initial guess was then updated using a damped Newton's method until the error in all equations dropped below 10^{-8}.

An important aspect of the solution that cannot be neglected is the details of the truncation of the integral. Keeping the arclength step, Δs, the same and increasing the truncation point s_N results in quite different looking solutions and very poor convergence. At small values of s_N with no surface tension, the results reproduce those seen in Forbes & Hocking (1990); Hocking et al. (2002) with smooth solutions rising to a maximum value of F_S at which a stagnation ring formed on the surface. Increasing s_N led to waves forming on the free surface that had ever-shortening wavelength, as determined by Vanden-Broeck & Keller (1997) in the infinite depth case. The problem with the truncation point is caused by the logarithmic nature of the kernel once the singular term is removed. Vanden-Broeck & Keller (1997) used a different scheme in which they integrated directly through the logarithmic singularity. While this avoids the problem with truncation, the numerical scheme converges very slowly as the step size is decreased, resulting in similarly inaccurate limiting solutions.

Thus, it is essential to include some approximation for that component of the integral from s_N to ∞. This was done by using an expanding grid of points and an approximation for $\phi(s)$ for large s. A fitted form of $\phi(s)$ and

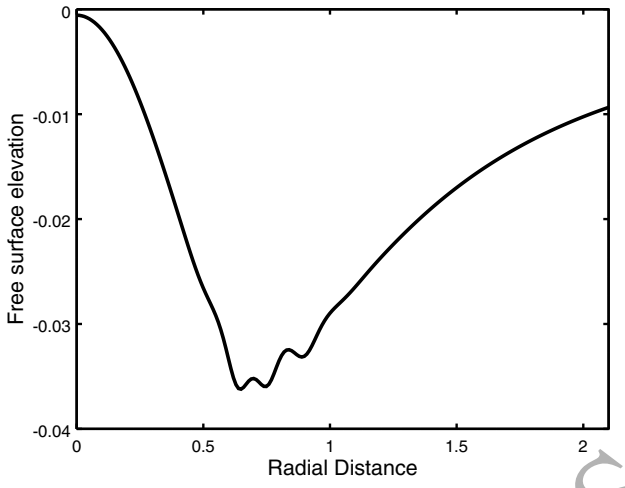

Figure 4: Limiting solution at $F_S = F_D = 1.8$ for $\beta = 0.001$ and $h_S = 1.0$. The ripples at the bottom of the dip are repeatable using both methods.

$\eta(s)$ allowed calculation of the truncated component out to extremely large distances.

This behaviour was described in more detail in the unbounded case by Hocking et al. (2015). Larger values of truncation resulted in increasing wave activity on the surface and a decrease in the maximum Froude number. Once convergence had been obtained, the limiting solutions were found to have no secondary stagnation ring and no wavelets on the surface, as in the case of infinite depth (Hocking et al. (2015)). This difficulty with the numerical schemes was greatly diminished by the inclusion of even moderate amounts of surface tension.

5. Calculations

Earlier attempts at solving this problem concentrated on the case of zero surface tension and considered the so-called "bottom-flux" case in which the point sink is located on the base of the fluid. Maximal flows were computed as $F_D = 3.2$ by Hocking et al. (2002) and $F_D = 1.25$ by Forbes et al.

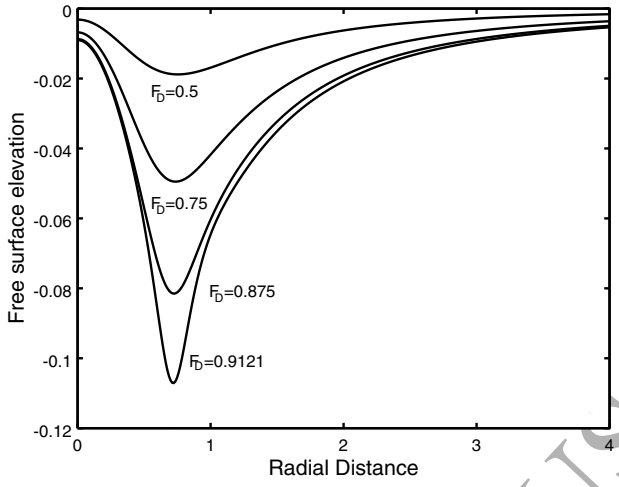

Figure 5: Free surface shapes for $\beta = 0.0025$ and $h_S = 0.75$ with $F_D = 0.5, 0.75, 0.875, 0.9121$ (limiting). Corresponding F_S values are $2.82, 4.24, 4.95$ and 5.16. The depth of the dip is rapidly increasing as F_S increases, a factor which may lead to the collapse of the steady solution.

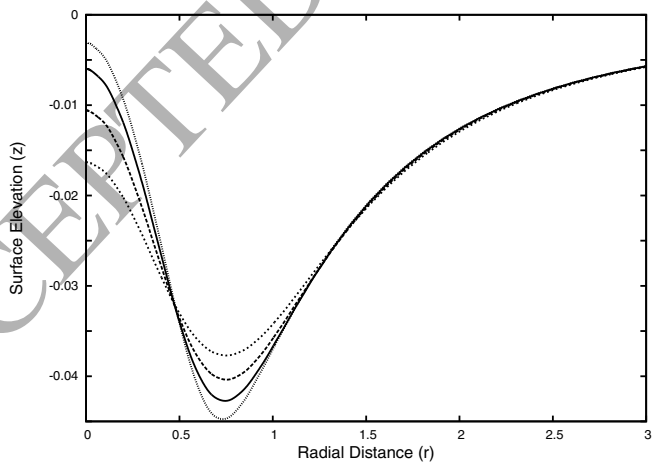

Figure 6: Free surface shapes for $\beta = 0.005, 0.01, 0.02, 0.04$ (Top to bottom at $r = 0$) with $F_D = F_S = 1.0$ for the case of the sink on the base. Higher surface tension leads to a lower stagnation point in the middle but a slightly shallower dip surrounding.

(1996) using a fundamental singularity method and Galerkin scheme. Here, simulations using the spectral method give a maximum $F_D \approx 1.5$, while the modified integral equation method gives a maximum Froude number of $F_D \approx 1.45$. When no surface tension is involved, however, both methods give high frequency (although small amplitude) jagged oscillations near the maximum value of F_S that are clearly numerical in origin, making it slightly difficult to determine the exact value.

Figure 3 shows a comparison between the results of the two methods for the case $h_S = 1/3$ and $F_D = 0.2$ ($F_S = 3.1$) with $\beta = 0$. The left panel is the integral equation solution, while the right panel shows the difference between the integral equation and the spectral solutions. Regular oscillations of the spectral method are combined with the more violent wiggles on the central pillar near $r = 0.08 - 0.1$ and on the upslope near $r = 0.6$. If the Froude number is increased beyond these values the oscillations become worse and the method fails to converge. In spite of this, it is clear that the two methods are giving very close to the same results, with the difference in surface height, even in this limiting case, of the order of 10^{-5}.

Further computations were conducted and resulted in a series of numerical solutions showing the influence of surface tension and sink depth on the critical, maximum Froude number. The inclusion of even a tiny amount of surface tension reduced the problems discussed above and it was much easier to obtain "matching" results. In the case with the sink on the bottom and surface tension as small as $\beta = 0.001$ the limiting spectral solution was at $F_D = 1.82$ and for the integral equation it was $F_D = 1.8$. An interesting limiting solution exists in this case in which there are ripples on the surface that seem not to be numerical in origin, as shown in Figure 4. They are repeatable using either method, but once β reaches 0.0025, they no longer appear.

Table 1 shows the maximal steady flow values of F_S for a range of surface

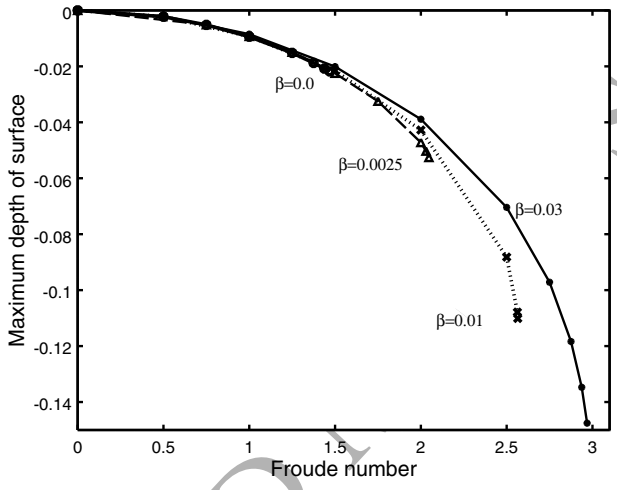

Figure 7: Maximum depth of the surface against $F_S = F_D$ for the sink on the bottom $h_S = 1$ for different values of surface tension $\beta = 0, 0.0025, 0.01, 0.03$. The depth is approximately the same for each Froude number and surface tension until the solutions get closer to the limiting steady flow. The sharp drop at the end as the maximum F_S is reached appears to suggest a rapid deepening of the free surface at higher values and may explain the breakdown of the steady solutions.

tension and sink depths. It appears that if there is zero surface tension ($\beta = 0$) then if the sink is at less than half of the depth of the channel the limiting value of $F_S \approx 3$ is about the same as the infinite depth case (Hocking et al. (2015)). However, as β increases this is no longer the case.

Figure 6 shows comparable free surface shapes at the same value of $F_S = F_D = 1$ for the bottom flux case ($h_S = 1$) at different values of surface tension β. It is clear that the only effects are near the central region, with the centre stagnation point getting deeper as β increases and the surrounding dip getting shallower.

The depth of the circular dip around the central rise is reasonably consistent in size. This can be seen more clearly in Figure 7 which plots maximum dip depth as F_S increases for different β. The curves follow a very similar path until they diverge as the maximum Froude number is approached. Interestingly the dip remains shallower for the higher surface tension values, but then dips more quickly as the critical value is approached, suggesting a rapid deepening of the free surface would occur at this point if F were slightly higher. This sudden increase in depth is clearly seen in Figure 5, which shows steady solutions for several different values of F_S. The last two values are only slightly different yet the surface dip is much deeper. A further illustration of this nonlinear effect can be seen in Figure 2 where the difference between the rigid-lid solution and full numerical solution consists mainly of the maximum depth reached by the free surface.

Surface tension has the effect of stabilizing the flow (and both numerical schemes) and reduces the distortion of the free surface at equivalent values of F_D so that higher values of Froude number exist as the surface tension increases. Figure 8 clearly demonstrates this effect, with the Froude number for steady flow plotted against surface tension, β. The smoothness of this curve as surface tension $\beta \to 0$ provides a strong case that the methods described in

h_S	$\beta = 0$	0.0025	0.005	0.01	0.02	0.03	0.04	0.05
1.00	1.45	2.06	2.30	2.55	2.80	2.96	3.05	3.14
0.75	2.55	3.28	3.99	4.44	4.56	4.85	5.01	5.21
0.50	3.15	5.16	5.66	6.11	6.68	6.96	7.13	7.30
0.33	3.12	6.00	6.63	7.09	7.64	8.03	8.42	8.73
0.20	3.10	7.04	7.27	7.94	9.11	9.78	10.40	10.90
0.10	3.16	7.30	7.60	9.64	12.06	13.64	14.82	15.50

Table 1: Maximum values of F_S for each sink depth and surface tension value, β. Agreement between the two methods is very good except for values of β very close to zero. The values here are taken from the integral equation approach.

this work are giving a consistent limit for the case of zero surface tension.

Moving the sink off the bottom also reduces the restriction of the flow and so at equivalent values of flow volume the speed is smaller, so it is to be expected that the maximum Froude number (based on sink depth, F_S) would increase. In the absence of surface tension this should approach the value obtained in the unconfined case ($F_S \approx 3$), and indeed this is so. In fact for $\beta = 0$ if the sink is located at less than half of the channel depth the flow matches the infinite depth case quite well. If one were to take the limit of infinite surface tension, the surface would be horizontal and would replicate the rigid lid solution, so it is to be expected that increasing surface tension would allow much larger flow rates, and this can be clearly seen in Table 1. With a large surface tension value of $\beta = 0.05$, the bottom-flux case gives a maximum $F_S \approx 3$ and in the infinite depth case it is approaching $F_S \approx 16$.

6. Conclusions

Two completely different numerical methods were used to compute the shape of a free surface affected by the flow into a point sink. These flows are

interesting from a pure free-surface hydrodynamics standpoint, but are also of use in understanding withdrawal flows from lakes and reservoirs. A range of different flow rates, sink depths and values of surface tension were considered. The numerical schemes were compared with a rigid-lid approximation for small flow rate with good agreement.

The spectral method is very similar to the Galerkin method used by Forbes et al. (1996), and produces results consistent with those. The results using the integral equation, when compared with older work, e.g. Forbes & Hocking (1990), emphasise the care that is needed in using this method on such axi-symmetric flow problems. The weak logarithmic singularity in the kernel must be treated with great care to get completely converged results. This is not an issue in the equivalent two dimensional flows where a slightly stronger pole singularity makes the numerical method more robust, e.g. Forbes & Hocking (1993).

Using the algorithms described the two methods gave the same surface shapes (to graphical accuracy) for all values of each parameter. The only difference in the results came in the limiting maximal value for the flow rate at which steady solutions could be obtained. However, in most cases these values agreed quite closely. The differences in the two schemes are most prominent as the surface tension decreases toward zero, as can be seen in Table 1 for the case of the sink on the bottom of the channel. Once $\beta > 0.0025$ it is clear that the two methods produce the same outcomes.

For values of $\beta < 0.0025$ the two methods give slightly different critical values for the limit on flow, but the difference is only in the first decimal place. At low surface tension values the limiting solutions are caused by small instabilities on the surface that appear as grid-dependent oscillations in the solution. However, at larger surface tension values the dip around the sink deepens rapidly as flow rate increases and it would appear that it is the sudden

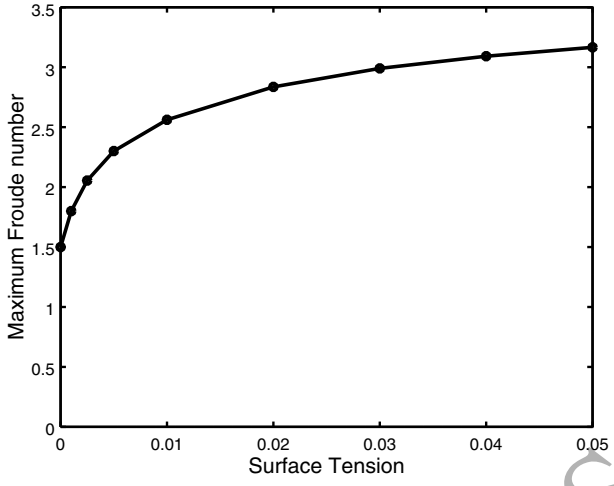

Figure 8: Maximum Froude number F_S with the sink on the base for increasing surface tension values.

deepening of the dip, perhaps as a precursor to drawdown, that leads to the limiting steady solution.

References

Abramowitz, M & Stegun, I. A. 1970 Handbook of Mathematical Functions, Dover, New York

Craya, A. 1949 Theoretical research on the flow of nonhomogeneous fluids, La Houille Blanche, 4, pp.44-55.

Forbes, L. K. & Hocking, G. C. 1990 Flow caused by a point sink in a fluid having a free surface, *J. Austral. Math. Soc. B* **32**, 231–249

Forbes, L. K. & Hocking, G. C. 1993 Flow induced by a line sink in a quiescent fluid with surface-tension effects, *J. Austral. Math. Soc.* Ser B. **34**, 377-391.

Forbes, L. K., Hocking, G. C. & Chandler, G. A. 1996 A note on withdrawal through a point sink in fluid of finite depth, *J. Austral. Math. Soc. Ser. B* **37**, 406–416.

Forbes, L. K. & Hocking, G. C. 2003 On the computation of steady axi-symmetric withdrawal from a two-layer fluid, *Computers and Fluids*, 32, 385–401, doi: 10.1017/S0022112098008805

Harleman, D. R. F, Morgan R. L. & Purple, R. A. 1959 Selective withdrawal from a vertically stratified fluid, in *Proc. Int. Assoc. Hyd. Res., 8th Congr, Montreal.*

Hocking, G. C. & Forbes, L. K. 1991 A note on the flow induced by a line sink beneath a free surface, *J. Austral. Math. Soc. Ser. B.* **32**, 251–260

Hocking, G. C. 1995 Supercritical withdrawal from a two-layer fluid through a line sink, *J. Fluid Mech.*, 297, 37–47.

Hocking, G.C. & Forbes, L.K. 2001 Supercritical withdrawal from a two-layer fluid through a line sink if the lower layer is of finite depth, *J. Fluid Mech.* 428, 333-348.

Hocking,G.C., Vanden Broeck, J.-M & Forbes,L.K. 2002 Withdrawal from a fluid of finite depth through a point sink, *ANZIAM J.*, 44, 181–191.

Hocking G.C., Forbes L.K. & Stokes T.E., 2014, A note on steady flow into a submerged point sink, *ANZIAM J.*, 56, 150–159 *doi:10.1017/S1446181114000303*

Hocking G.C., Nguyen H.H.N., Forbes L.K. & Stokes T.E., 2016, The effect of surface tension on free surface flow induced by a point sink, *ANZIAM J.*, 57, 417–428, *doi:10.1017/S1446181116000018*

Holmes, R. J. & Hocking G. C., 2015, A line sink in a flowing stream with surface tension effects, *Euro. J. Applied Math.*, 27, pp 248-263, doi:10.1017/S0956792515000546

Imberger, J. & Hamblin, P. F. 1982 Dynamics of lakes, reservoirs and cooling ponds, *Ann. Rev. Fluid Mech.*, 14, 153–187.

Imberger, J. & Patterson, J. C. 1990, Physical Limnology. *In: Advances in Applied Mechanics*, Hutchinson, J.W. and Wu, T. (eds.), Academic Press, Boston, 27, 303–475.

Jirka, G. H. & Katavola, D. S. 1979 Supercritical withdrawal from two-layered fluid systems, Part 2 -Three dimensional flow into a round intake, *J. Hyd. Res.*, 17(1), 53–62.

Lubin B. T. & Springer, G. S. 1967 The formation of a dip on the surface of a liquid draining from a tank, *J. Fluid Mech.*, **29**, 385-390.

Miloh T. & Tyvand P. A 1993 Nonlinear transient freesurface flow and dip formation due to a point sink, *Phys. Fluids A* **5**, 1368 http://dx.doi.org/10.1063/1.858572

Peregrine, H. 1972 A line source beneath a free surface, *Rept. No. 1248, Math Res. Centre,* University of Wisconsin, Madison.

Sautreaux, C. 1901 Mouvement d'un liquide parfait soumis à la pesanteur. Dé termination des lignes de courant, *J. Math. Pures Appl.* **7** (5), 125–159.

Stokes, T. E., Hocking, G. C. & Forbes, L. K., 2003, Unsteady free-surface flow induced by a line sink, *J.Eng.Maths*, 47, 137-160.

Stokes, T. E., Hocking, G. C. & Forbes, L. K. 2005 Unsteady flow induced by a withdrawal point beneath a free surface, *ANZIAM J.* **47**, 185–202.

Stokes, T. E, Hocking, G. C. & Forbes, L. K., 2008, "Unsteady flow induced by a line sink in a fluid of finite depth", *Computers & Fluids*, 37, 236-249

Tuck, E. O. & Vanden Broeck, J-M. 1984 A cusp-like free surface flow due to a submerged source or sink, *J. Austral. Math. Soc. Ser. B* **25**, 443–450.

Vanden Broeck, J.-M. & Keller, J.B. 1987 Free surface flow due to a sink, *J. Fluid Mech.* **175**, 109–117

Vanden Broeck, J.-M. & Keller, J. B. 1997 An axisymmetric free surface with a 120 degree angle along a circle, *J. Fluid Mech.*, 342:403-409. DOI: 10.1017/S0022112097005892

Xue, X. & Yue, D. K. P 1998 Nonlinear free-surface flow due to an impulsively started submerged point sink, *J. Fluid Mech.* **364**, 325–347.

Zhou, Q & Graebel, W. P., 1990 Axisymmetric draining of a cylindrical tank with a free surface, *J. Fluid Mech.*, 221, 511-532.